Enhanced Image Resolution and Reduced Measurement Time Using Inner Volume Imaging and Parallel Excitation

J. T. Schneider[1,2], M. Haas[2], J. Hennig[2], S. Junge[1], W. Ruhm[1], and P. Ullmann[1]

[1]Bruker BioSpin MRI GmbH, Ettlingen, Germany, [2]Dept. of Diagnostic Radiology, Medical Physics, University Hospital Freiburg, Freiburg, Germany

Introduction: The basic principle of inner volume imaging, which is the restricted excitation and acquisition of NMR signals of a specific region of interest, was already described in 1985 [1]. Applications are e.g. the suppression of motion artifacts or the reduction of the field of view (FOV) to a given region without the risk of aliasing signals from sources outside this region. In first approaches to spatially selective signal generation, multiple perpendicular, slice selective excitation and refocusing pulses were applied. The limitation that only the selection of cuboidal volumes is possible with this technique could be overcome in principle by spatially selective excitation (SSE) with multidimensional RF pulses, as presented in 1989 [2]. But since pulse durations in such experiments are in the range of tens of milliseconds their application, especially in-vivo, is very limited. However, the use of multiple transmit coils and parallel excitation (PEX) / TransmitSENSE [3,4] offers the possibility to reduce pulse durations to a few milliseconds. In this study, PEX is applied to SSE of arbitrarily shaped regions in phantoms, fruit and in-vivo. The possibility of reducing measurement time and / or increasing spatial resolution by constraining the FOV to regions of interest is presented and the behavior of the signal-to-noise ratio (SNR) and of outer volume suppression is discussed.

Materials and Methods: The experiments were carried out with an 8-TX-channel 9.4 T, 30 cm bore BioSpec system (Bruker BioSpin MRI GmbH, Ettlingen, Germany) in combination with an 8-element TX/RX volume array with elements in classical loop design. As k-space trajectory a constant density, constant angular velocity spiral was chosen and PEX RF-pulses were calculated by the conjugate gradient method, described by Graesslin et al [5], with an acceleration factor of 2 and a pulse duration of 8.5 ms. As measurement objects we used a spherical phantom with T_1-doped saline water solution, a kiwi fruit and a Fischer rat for in-vivo evaluations. Each study was based on a pilot scan in which a region of interest was defined interactively. PEX pulses were calculated for exciting only this region and in the following PEX experiments first the entire section through the object, then a reduced FOV, covering the excited region, were imaged.

Because for in-vivo experiments mainly short measurement times are important the resolution of the rat pilot image was kept for the reduced-FOV image, thus reducing the number of phase encoding steps (and acquisition points in read direction) which resulted in a measurement time shortened by the same factor. For imaging a 2D RARE sequence was used in which the standard excitation pulse had been substituted by a parallel SSE module. In the kiwi images another approach was chosen, since measurement time is typically less critical in this case, just as in phantom experiments: The number of acquired data points was kept constant and since the imaging FOV was reduced in read and phase direction by a certain factor, a gain in resolution by the same factor could be achieved for an unchanged measurement time. Excitation and acquisition were performed in a 3D gradient-echo scan, also containing the modified excitation module.

For investigating the SNR and artifact behavior in images with reduced FOV, a square pattern was excited in the water phantom and a series of images with different sizes of the FOV were acquired. After repeating this series without playing out excitation pulses, thus generating pure noise images, the SNR was calculated for each case from the mean signal intensity within the defined square pattern and the signal standard deviation in the same region of the noise image. The result was compared with the theoretically expected values which depend, among others, on the voxel's volume V and the number of data points (N_r=N_p=N) in read and phase direction:

$$SNR \propto \sqrt{N_R \cdot N_p} \cdot V = FOV/N. \qquad \text{(Eq. 1)}$$

Excitation accuracy and intensity of backfolding artifacts in the case of FOV reduction were evaluated based on the full-FOV phantom image in Fig.3a: In the post-processing the FOV was virtually reduced point by point and new images with backfolded signals and artifacts were computed. For each step of reduction the difference image between this computed image and the corresponding part of the original full-FOV image was calculated resulting in a map of backfolding artifacts. A "signal to artifact ratio", describing the global distortion of the image by backfolded signal, was calculated from the mean image intensity in the excited region and the mean artifact map intensity (from which the noise level was subtracted in a further step) in this region.

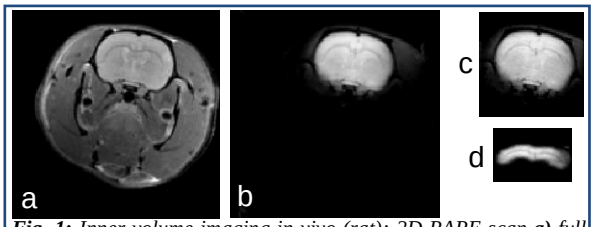

Fig. 1: *Inner volume imaging in-vivo (rat): 2D RARE scan* ***a)*** *full slice* ***b)*** *selectively excited brain* ***c)*** *FOV constrained to brain, acquired with unchanged resolution in half measurement time* ***d)*** *selectively excited corpus callosum imaged within a fourth of the original measurement time.*

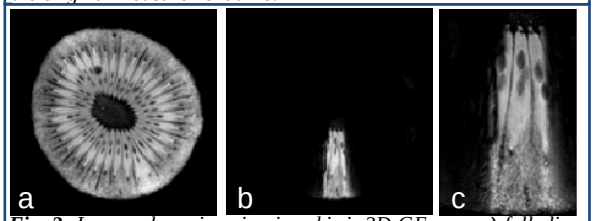

Fig. 2: *Inner volume imaging in a kiwi: 3D GE scan* ***a)*** *full slice* ***b)*** *selectively excited segment* ***c)*** *FOV constrained to segment, acquired with resolution enhanced by factor 4 in unchanged measurement time.*

Results and Discussion: Fig. 1a shows the scan of a complete slice through the rat's head, acquired within 94 s, with a FOV of $(3.8\ cm)^2$ and 128 data points in read and phase direction, resulting in an in-plane resolution of $(0.3\ mm)^2$. Within this image the brain was selected as region of interest and was selectively excited: Fig. 1b. Since excitation accuracy and suppression of signal generation outside the defined region were very good, the FOV could be centered to the brain and constrained by a factor of two in each direction to $(1.9\ cm)^2$. Keeping the resolution constant meant a reduction of data points in read and phase direction to 64 resulting in Fig. 1c which was acquired in 48 s - the half measurement time as in Fig. 1a+b. Finally even smaller and irregularly shaped structures like the corpus callosum were excited (Fig. 1d) and in this case, the number of phase encoding steps and measurement time could be reduced by a factor of 4.

In case of the kiwi, a 3D gradient-echo scan was performed whose central section is shown in Fig. 2a. Imaging parameters of this section were FOV=$(6.4\ cm)^2$, matrix size=128^2, in-plane resolution = $(0.5\ mm)^2$, measurement time = 238 s. Focusing on one segment of the kiwi (Fig 2b), zoomed imaging was performed: In this case the FOV was reduced by a factor of 4 in phase direction. Since the number of phase encoding steps was kept constant, the in-plane image resolution was increased by a factor of 4 to $(0.13\ mm)^2$ for unchanged measurement time, resulting in the image of Fig. 2c with nicely depicted structures.

The reduction of the number of phase encoding steps or of the voxel size is limited by decreasing SNR (Eq.1). In the image series of the water phantom with successively reduced FOV, the experimentally measured relative SNR_{exp} values were in very good agreement with the theoretically predicted SNR_{theo} decay (Fig. 3, Tab. 1) and no additional losses of SNR were observed.

The ratio of potential backfolding artifacts depending on the size of the FOV was examined based on the image of Fig. 3a showing the selectively excited square of 32^2 pixels with full FOV. Of course, FOVs smaller than the pattern's size of 32^2 pixels would lead to strong distortions in the image. Taking into account only FOVs completely covering the pattern, the signal-to-artifact ratio was calculated to be in the range of 70, i.e. the mean intensity of backfolding artifacts amounts to only 1.5% of the image intensity indicating a very good excitation accuracy in the phantom.

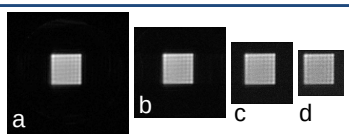

image	a	b	c	d
FOV / cm^2	6.4^2	4.8^2	3.2^2	2.4^2
rel. FOV	1	$(3/4)^2$	$(1/2)^2$	$(3/8)^2$
SNR_{exp}	133	75	33	19
rel. SNR_{exp} / %	**100**	**56**	**25**	**14**
rel. $SNRt_{heo}$ / %	**100**	**56**	**25**	**14**

Fig. 3, Tab. 1: *Selectively excited square pattern in the water phantom in series with different FOVs for SNR calculation.*

Conclusion: This study evaluates the application of parallel spatially-selective excitation for inner volume imaging. Very good excitation accuracy allows constraining the FOV to specific regions of interest without additional losses in SNR beyond the theoretical predictions. With PEX inner volume imaging of regions of interest can be performed with significant reduction of measurement time and / or with highly enhanced image resolution.

References and Acknowledgement: 1. Feinberg DA et al. (1985) Radiology 156:743 // **2.** Pauly J et al. (1989) JMR 81:43 // **3.** Katscher U et al. (2003) MRM 49:144 // **4.** Ullmann P et al. (2005) MRM 54:994 // **5.** Graesslin I. et al. (2006) Proc. ISMRM 2006:2470 // This work is part of the INUMAC project supported by the German Federal Ministry of Education and Research. Grant #13N9207. Special thanks to Ute Molkentin, Anita Siebert and Andreas Steingötter for support in experiments and animal handling.